Journal of the Optical Society of Korea
Vol. 20, No. 3, June 2016, pp. 431-434

ISSN: 1226-4776(Print) / ISSN: 2093-6885(Online)
DOI: http://dx.doi.org/10.3807/JOSK.2016.20.3.431

High-precision THz Dielectric Spectroscopy of Tris-HCl Buffer

Soonsung Lee[1], Hyeona Kang[1], Youngwoong Do[1], Gyuseok Lee[1], Jinwoo Kim[2], and Haewook Han[1]*

[1]*Department of Electrical Engineering, POSTECH, San 31, Hyoja-dong, Namgu, Pohang 790-784, Korea*
[2]*Department of Biological and Agricultural Engineering, Institute for Nanoscience and Engineering, University of Arkansas, Fayetteville, AR 72701, USA*

(Received April 29, 2016 : revised May 27, 2016 : accepted June 1, 2016)

Tris-HCl buffer solution is extensively used in biochemistry and molecular biology to maintain a stable pH for biomolecules such as nucleic acids and proteins. Here we report on the high-precision THz dielectric spectroscopy of a 10 mM Tris-HCl buffer. Using a double Debye model, including conductivity of ionic species, we measured the complex dielectric functions of Tris-HCl buffer. The fast relaxation time of water molecules in Tris-HCl buffer is ~20% longer than that in pure water while the slow relaxation time changes little. This means that the reorientation dynamics of Tris-HCl buffer with such a low Tris concentration is quite different from that of pure water.

Keywords : THz time-domain spectroscopy, Debye relaxation, Tris-HCl buffer
OCIS codes : (300.6495) Spectroscopy, terahertz; (160.1435) Biomaterials; (060.0060) Fiber optics and optical communications

I. INTRODUCTION

Biological buffer solution, a mixture of weak acid and its conjugate base, is used to maintain pH when a moderate amount of acid and base is added to it. Tris-HCl buffer is one of the most widely used buffers in biochemistry and molecular biology because of its high stability and compatibility [1]. In particular, Tris-HCl buffer in the range of pH 7.0-9.0 has been used as a neutralizing buffer to maintain optimum pH for various biological processes such as unzipping and hybridization of DNA [2], conformational dynamics of DNA including bending, cleavage and breathing processes of enzymatic proteins [3-5]. For biomedical applications, Tris-HCl buffer has also been used in sequence-specific DNA biosensors and protein biochips for disease screening and diagnosis [6-11].

THz dielectric spectroscopy (THz-TDS) has recently been used to study spectroscopic information of various biomolecules and biomedical tissues since it can probe molecular vibration and hydration dynamics of biomolecules such as RNA, DNA, and proteins [12-15]. Almost all of these THz measurements have been performed in biological buffers, not in pure water. However, in spite of the physiological importance of pH environment, there have been only a few studies on biological buffers at THz frequencies [16-18], and the THz dielectric property of Tris-HCl buffer has not been reported so far. The biochemical change of solute molecules in a buffer solution usually yields only a small difference in the THz dielectric property of an aqueous solution. For example, with commonly encountered dilute DNA solutions, it is very challenging to probe the conformational changes of DNAs and proteins by THz-TDS. The THz permittivity is usually obtained from THz transmission coefficient using a theoretical model based on effective medium approximation where bio-molecules with hydration layers (inclusions) are randomly distributed in a buffer solution (background medium) [19-21]. Therefore, it is necessary to precisely characterize the THz dielectric properties of the buffer solution, especially for a low concentration of biomolecules. In this work, we performed high-precision THz-TDS to obtain THz complex dielectric functions of Tris-HCl buffer and pure water.

*Corresponding author: hhan@postech.ac.kr
Color versions of one or more of the figures in this paper are available online.

II. EXPERIMENTAL RESULTS AND DISCUSSION

We used purified water (DEPC-treated and sterile filtered, Sigma Aldrich) to prepare 10 mM Tris-HCl buffer solution with a pH of 7.4 at 25℃. THz pulses were generated using an InAs wafer pumped by a Ti:sapphire laser with a pulse width of 100 fs, and detected by a photoconductive antenna fabricated on a low-temperature-grown GaAs substrate. A quartz liquid cell was placed at the focal point of the THz beam between two off-axis parabolic mirrors in a transmission geometry. To prevent the absorption of THz radiation by atmospheric water vapor, the entire THz-TDS system was enclosed in a chamber that was continuously purged with dry air during the measurements.

The liquid cell consists of two fused quartz plates with a small gap. The THz absorption of water has a strong absorption coefficient (~200 cm^{-1} at 1 THz), and the gap thickness should be chosen carefully to ensure high sensitivity of THz-TDS. In this work, we used a 50 μm gap for the optimum sensitivity of THz-TDS. As a calibration procedure, we first measured THz transmission coefficient of the liquid cell with an air gap to obtain the THz complex dielectric functions of the fused quartz by using transfer matrix analyses [22]. The thicknesses of the fused quartz and air gap were simultaneously determined in a self-consistent manner using a least-square method based on the Levenberg-Marquardt algorithm [23]. From these calibration data, we measured the THz complex dielectric functions of Tris-HCl buffer and pure water. We used an extended double Debye model, including conductivity of ionic species (Tris-H^+ and Cl^-), to obtain the slow and fast relaxation times of water molecules in the buffer and pure water.

Figure 1(a) shows the THz pulse signals transmitted through the liquid cell with water and Tris-HCl buffer. The THz pulse for Tris-HCl buffer is delayed by ~70 fs and the positive peak is reduced by 0.3 nA, compared with that for water, which means that the Tris-HCl buffer has slightly higher refractive index and absorption coefficient. The fast Fourier transformed (FFT) amplitude and phase spectra in Fig. 1(b) and 1(c) also show very small differences between the two liquids, demonstrating the high precision of our measurements.

We obtained the complex dielectric functions using a double-Debye model with slow and fast relaxation processes [24], including conductivity of solute ions such as Tris-$H^+$and Cl^-:

$$\varepsilon(\omega)=\frac{S_1}{1-i\omega\tau_1}+\frac{S_2}{1-i\omega\tau_2}+\frac{\sigma}{i\omega\varepsilon_0}+\varepsilon_\infty \tag{1}$$

with the real (ε_1) and imaginary (ε_2) parts given by

$$\begin{aligned}\varepsilon_1(\omega)&=\frac{S_1}{1+(\omega\tau_1)^2}+\frac{S_2}{1+(\omega\tau_2)^2}+\varepsilon_\infty\\ \varepsilon_2(\omega)&=\frac{\omega\tau_1 S_1}{1+(\omega\tau_1)^2}+\frac{\omega\tau_2 S_2}{1+(\omega\tau_2)^2}+\frac{\sigma}{\omega\varepsilon_0}\end{aligned} \tag{2}$$

where ω is the angular frequency, S_1 (S_2) and τ_1 (τ_2) are the dielectric strength and relaxation time of the slow (fast) relaxation process, respectively, ε_0 and ε_∞ are the static and high-frequency permittivities, respectively, and σ is the conductivity of ionic species.

As shown in Figs. 2(a) and 2(b), the measured complex dielectric functions are in good agreement with the best-fit curves for both water and Tris-HCl buffer. At 1 THz, the real and imaginary parts (ε_1 and ε_2) of the complex dielectric function of the Tris-HCl buffer are ~ 10% and 4% larger than those of water, respectively. This is because the ionic components in the Tris-HCl buffer decrease the dielectric strengths (S_1 and S_2) and increase the relaxation times (τ_1 and τ_2) due to the hydration shell around the ionic components. We also obtained the refractive indices and absorption coefficients from the complex dielectric function as shown in Fig. 2(c) and 2(d). Although we used a dilute buffer with a low Tris concentration, [Tris-H^+] /[H_2O] = 1.80×10^{-4}, we observed the clear distinction between complex dielectric functions of two liquids. This is in sharp contrast with a previous result [16] where any measurable difference between

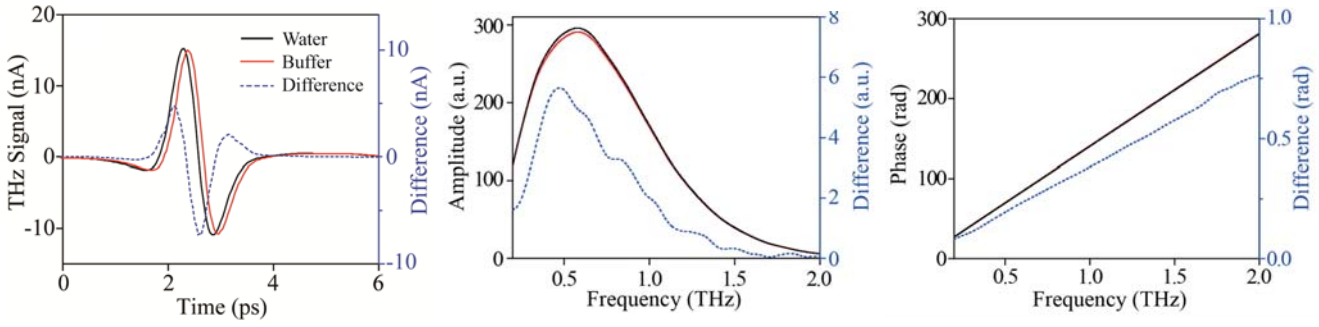

(a) (b) (c)

FIG. 1. (a) THz pulse signals of water and Tris-HCl buffer and the difference signal. (b), (c) THz amplitude and phase spectra of Tris-HCl buffer and water, and the difference spectrum (dashed blue).

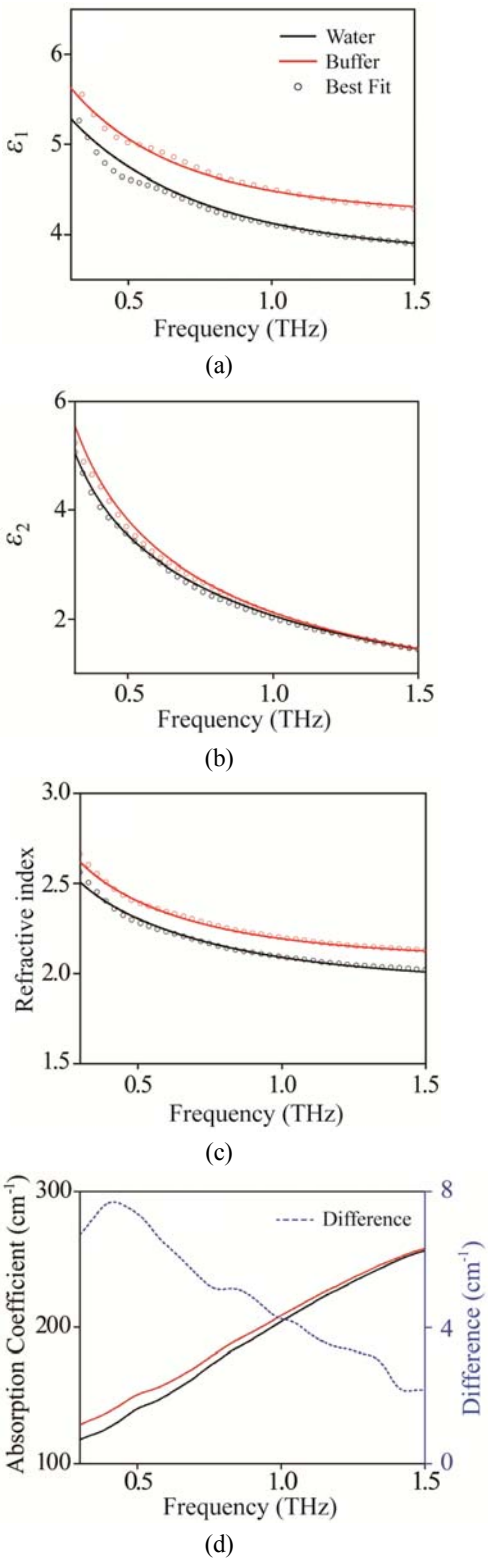

FIG. 2. (a), (b) Real and imaginary parts of THz complex permittivities (open circles) and their best-fit curves (solid lines) of water (black) and Tris-HCl buffer (red). (c) Refractive indices (open circles) and the best-fit curves (solid line) of water (black) and Tris-HCl buffer (red). (d) Absorption coefficients of water (black), Tris-HCl buffer (red) and the difference (dashed blue).

TABLE 1. Dielectric relaxation parameters of water and Tris-HCl buffer

	Water	Tris-HCl (0.01M)
S_1	75.9	74.4
τ_1	9.30	9.31
S_2	1.73	1.72
τ_2	0.274	0.327
σ (Ω^{-1}cm^{-1})	0	11.3
ε_∞	3.67	4.14

phosphate buffer and water was not observed even with a higher concentration (50 mM) of potassium phosphate. Table 1 shows the best-fit Debye parameters and conductivity, where S_1 decreases by ~ 2% and τ_2 increases by ~20% for 10 mM Tris-HCl buffer compared to water.

III. CONCLUSION

We have performed high-precision THz time-domain spectroscopy of 10 mM Tris-HCl buffer and water. The measured and best-fit complex dielectric functions have shown the difference between the two liquids very clearly even with a dilute Tris-HCl buffer solution. These findings suggest that the high-precision THz-TDS is a powerful spectroscopic tool for probing various biochemical processes even in physiological buffer solutions.

ACKNOWLEDGMENT

This study was supported by the Basic Science Research Program (2009-0083512), and the Priority Research Centers Program (2010-0029711) through the National Research Foundation of Korea (NRF), funded by the Ministry of Education, Science and Technology, Korea and the Brain Korea 21 Project, and by the IT Consilience Creative Program (C1515-1121-0003).

REFERENCES

1. G. Gomori, "Buffers in the range of pH 6.5 to 9.6," Exp. Biol. Med. **62**, 33-34 (1946).
2. A. Shundrovsky, C. L. Smith, J. T. Lis, C. L. Peterson, and M. D. Wang, "Proving SWI/SNF remodeling of the nucleosome by unzipping single DNA molecules," Nat. Struct. Mol. Biol. **13**, 549-554 (2006).
3. M. I. Wallace, L. Ying, S. Balasubramanian, and D. Klenerman, "FRET Fluctuation Spectroscopy: exploring the conformational dynamics of a DNA hairpin loop," J. Phys. Chem. B. **104**, 11551-11555 (2000).
4. T. Bentin and P. E. Nielsen, "Enhanced peptide nucleic acid binding to supercoiled DNA: possible implications for

DNA "breathing" dynamics," Biochem. **35**, 8863-8869 (1996).
5. T. Tanaka and H. Hidaka, "Hydrophobic regions function in calmodulin-enzyme(s) interactions," J. Biol. Chem. **255**, 11078-11080 (1980).
6. J. Wang, E. Palecek, P. E. Nielsen, G. Rivas, X. Cai, H. Shiraishi, N. Dontha, D. Luo, and P. A. M. Farias, "Peptide nucleic acid probes for sequence-specific DNA biosensors," J. Am. Chem. Soc. **118**, 7667-7670 (1996).
7. P. Arenkov, A. Kukhtin, A. Gemmell, S. Voloshchuk, V. Chupeeva, and A. Mirzabekov, "Protein microchips: use for immunoassay and enzymatic reactions," Anal. Biochem. **278**, 123-131 (2000).
8. Z. Chang, H. Fan, K. Zhao, M. Chen, P. He, and Y. Fang, "Electrochemical DNA biosensors based on palladium nanoparticles combined with carbon nanotubes," Electroanal. **2**, 131-136 (2008).
9. Y. Heyman, A. Buxboim, S. G. Wolf, S. S. Daube, and R. H. Bar-Ziv, "Cell-free protein synthesis and assembly on a biochip," Nat nanotechnol. **7**, 374-378 (2012).
10. S. Siddiquee, K. Rovina, N. A. Yusof, and K. F. Rodrigues, "Nanoparticle-enhanced electrochemical biosensor with DNA immobilization and hybridization of Trichoderma harzianum gene," Sens. Biosens. Res. **2**, 16-22 (2014).
11. A. Ulianas, L. Y. Heng, M. Ahmad, H. Y. Lau, Z. Ishak, and T. L. Ling, "A regenerable screen-printed DNA biosensor based on acrylic microsphere-gold nanoparticle composite for genetically modified soybean determination," Sens. Actuators B **190**, 694-701 (2016).
12. P. H. Siegel, "Terahertz technology in biology and medicine," IEEE Trans. Microwave Theory Tech. **52**, 2438-2446 (2004).
13. J. Son, "Terahertz electromagnetic interactions with biological matter and their applications," J. Appl. Phys. **105**, 102033 (2009).
14. B. M. Fischer, M. Walther, and P. Uhd Jepsen, "Far-infrared vibrational modes of DNA components studied by terahertz time-domain spectroscopy," Phys. Med. Biol. **47**, 3807-3814 (2002).
15. A. G. Markelz, J. R. Knab, J. Y. Chen, and Y. He, "Protein dynamical transition in terahertz dielectric response," Chem. Phys. Lett. **442**, 413-417 (2007).
16. J. Xu, K. W. Plaxco, and S. J. Allen, "Absorption spectra of liquid water and aqueous buffers between 0.3 and 3.72 THz," J. Chem. Phys. **124**, 036101 (2006).
17. B. Born, S. J. Kim, S. Ebbinghaus, M. Gruebele, and M. Havenith, "The terahertz dance of water with the proteins: the effect of protein flexibility on the dynamical hydration shell of ubiquitin," Faraday. Discuss. **141**, 161-173 (2009).
18. S. Oh, J. Son, O. Yoo, and D. Lee, "Terahertz characteristics of electrolytes in aqueous Luria-Bertani media," J. Appl. Phys. **102**, 074702 (2007).
19. A. Sihvola. *Electromagnetic Mixing Formulas and Applications* (IET Electromagnetic Waves Series 47, London, 1999).
20. L. L. Latour, K. Svoboda, P. P. Mitra, and C. H. Sotak, "Time-dependent diffusion of water in a biological model system," Proc. Natl. Acad. Sci. **91**, 1229-1233 (1994).
21. E. M. Johnson, D. A. Berk, R. K. Jain, and W. M. Deen, "Hindered Diffusion in Agarose Gels: Test of Effective Medium Model," Biophys. J. **70**, 1017-1026 (1996).
22. S. L. Chuang, *Physics of Optoelectronic Devices* (Wiley, 1995).
23. D. W. Marquardt, "An algorithm for least-squares estimation of nonlinear parameters," J. Soc. Indust. Appl. Math. **11**, 431-441 (1963).
24. M. Koeberg, C. C. Wu, D. Kim, and M. Bonn, "THz dielectric relaxation of ionic liquid: water mixtures," Chem. Phys. Lett. **439**, 60-64 (2007).